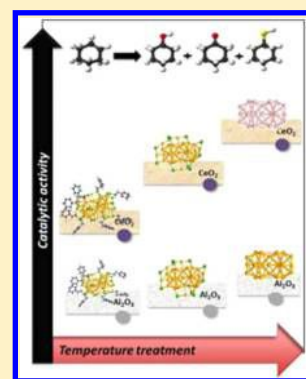


Modulation of Active Sites in Supported  $\text{Au}_{38}(\text{SC}_2\text{H}_4\text{Ph})_{24}$  Cluster Catalysts: Effect of Atmosphere and Support MaterialB. Zhang,<sup>†</sup> S. Kaziz,<sup>‡</sup> H. Li,<sup>§</sup> M. G. Hevia,<sup>||</sup> D. Wodka,<sup>†</sup> C. Mazet,<sup>§</sup> T. Bürgi,<sup>\*,†</sup> and N. Barrabés<sup>\*,†</sup><sup>†</sup>Department of Physical Chemistry, University of Geneva, Geneva, Switzerland<sup>‡</sup>Department of Industrial Engineering, National High School of Engineers of Tunis, Tunis, Tunisia<sup>§</sup>Department of Organic Chemistry, University of Geneva, Geneva, Switzerland<sup>||</sup>Institute of Chemical Research of Catalonia (ICIQ), Tarragona, Spain

## S Supporting Information

**ABSTRACT:** We investigate the distinctly different interaction of thiolate-protected cluster  $\text{Au}_{38}(\text{SC}_2\text{H}_4\text{Ph})_{24}$  with two diverse support materials  $\text{Al}_2\text{O}_3$  and  $\text{CeO}_2$ . The catalytic surfaces have been heated in different atmospheres, and the removal of the thiolate ligands has been studied. Thermogravimetry (TG), temperature-programmed process coupled with mass spectrometer (TPRDO-MS), and X-ray absorption spectroscopy (XAFS) studies were performed to understand the desorption of thiol ligands depending on conditions and support material. Depending on the atmosphere and the support material the fate of the thiol ligands is different upon heating, leading to metallic Au in the case of  $\text{Al}_2\text{O}_3$  and to cationic Au with  $\text{CeO}_2$ . The thiolate removal seems to be a two-step procedure. The catalytic activity of these  $\text{Au}_{38}$ -supported clusters was studied for the aerobic oxidation of cyclohexane. Conversion was higher for the gold clusters supported on  $\text{CeO}_2$ . Surprisingly, a significant amount of cyclohexanethiol was found, revealing the active participation of the thiolate ligand in catalytic reactions. The observation also indicates that breaking and formation of C–S bonds can be catalyzed by the gold clusters.



## ■ INTRODUCTION

Heterogeneous catalytic processes by supported thiolate-protected clusters ( $\text{Au}_n(\text{SR})_m$ ) represent an emerging field stimulated by reports showing higher activity and selectivity in several oxidation reactions<sup>1–4</sup> in comparison with metal nanoparticle catalysts. These clusters consist of a symmetric metal core protected by multiple gold–thiolate staples  $-\text{SR}-$  ( $\text{Au}-\text{SR}-$ )<sub>n</sub> ( $n = 1, 2$ ) that present size-dependent physical chemical properties, related with their quantized electronic structure and unique geometrical structure. In comparison to bulk gold, which has a face-centered cubic (fcc) structure, clusters of sizes <2 nm often show icosahedral structure.<sup>5</sup>

Thiolate-protected clusters represent atomically well-defined active centers for catalysis with resolved crystal structure, allowing one to create a homogeneous and defined surface. However, the thiol ligands around the Au core of these clusters are known to form strong Au–S bonds, which interfere with the catalytic properties by blocking or poisoning the active site. In addition, some of the physicochemical properties of clusters are directly related to the adsorbate such as chirality, electronic structure, and stability. In this sense different properties can be expected after ligand removal from the clusters. Experimentally, heating and reduction are common methods to control the surface coverage of thiolates on gold nanoclusters. Previous studies have shown relevant changes in the catalytic behavior of supported  $\text{Au}_n(\text{SR})_m$  related with the partial or complete removal of the thiol ligands around the metal core. Thiolate-protected Au nanoclusters exhibited enhanced catalytic activity

and selectivity upon gradual ligand removal in CO oxidation,<sup>6</sup> aerobic alcohol oxidation,<sup>7</sup> and styrene oxidation.<sup>4</sup> The intact clusters, however, showed low or even no catalytic activity.<sup>3,7</sup> Removal of the protecting ligands reduces surface steric hindrance. In addition, the decrease of reducing thiolate ligands improved the oxidation ability of the Au nanocluster.<sup>1</sup> More importantly, catalytic active sites are exposed after ligand desorption. CO oxidation was favored by thermally treated  $\text{Au}_{25}(\text{SR})_{18}/\text{CeO}_2$  clusters in which Au was exposed to CO absorption.<sup>8</sup>

Most catalytic reactions reported so far have been carried out with  $\text{Au}_{25}(\text{SR})_{18}$  clusters supported on materials such as  $\text{CeO}_2$ ,  $\text{TiO}_2$ , and multiwall carbon nanotubes. Immobilized Au nanoclusters on support materials possess uniformity and can be easily recovered from aqueous reaction mixtures. Nevertheless, such composite oxidation catalysts exhibit some drawbacks related to the active species and reaction sites, and various efforts have been made to address these issues. First of all, it has been observed that the catalytic activity varies with the type of support material in CO oxidation,<sup>3</sup> sulfide oxidation,<sup>2</sup> and aerobic alcohol oxidation.<sup>7</sup> The reducible oxide supports such as  $\text{CeO}_2$  enable oxygen adsorption, which gives high

**Special Issue:** Current Trends in Clusters and Nanoparticles Conference

**Received:** December 2, 2014

**Revised:** March 20, 2015

**Published:** March 20, 2015



catalytic oxidation activity and reduced selectivity. In addition, supported clusters after treatment in different atmosphere ( $\text{H}_2$ ,  $\text{O}_2$ ,  $\text{N}_2$ , and so on) were used to perform oxidation reaction.<sup>3</sup> Interestingly,  $\text{O}_2$  pretreatment favored the CO oxidation by creating active oxygen species and by changing the charge state of metal atoms. Controlled removal of thiolate ligands from supported clusters was studied by DRIFTS, EXAFS, and TPO.<sup>6,8,9</sup>  $\text{CeO}_2$ -supported  $\text{Au}_{25}$  nanoclusters showed a two-step thiolate desorption process by heating at 175 and 200 °C, which has been assigned to the two types of Au–S bonding modes in the thiolate-protected  $\text{Au}_{25}$  cluster.<sup>8–10</sup> Upon complete ligand removal, no aggregation was observed, while sintering appeared at higher temperature. In situ DRIFTS revealed that three types of active Au sites for CO oxidation were exposed after complete ligand removal. Despite the understanding on  $\text{Au}_{25}$  catalysis obtained so far, catalytic studies with other gold cluster sizes in oxidation reactions still remain a challenge.

Among the well-studied nanoclusters,  $\text{Au}_{38}(\text{SR})_{24}$  shows unique structure and properties. The total structure was solved by X-ray crystallography.<sup>11</sup> The  $\text{Au}_{38}(\text{SR})_{24}$  nanocluster comprises a symmetric  $\text{Au}_{23}$  core, and the core is protected by three monomeric staples SR–Au–SR and six dimeric staples SR–Au–SR–Au–SR (Figure 1). Interestingly,  $\text{Au}_{38}(\text{SR})_{24}$

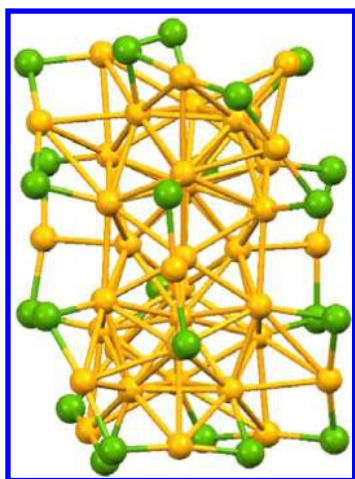


**Figure 1.**  $\text{Au}_{38}(\text{SR})_{24}$  cluster structure (Au: yellow; S: green). The thiolate ligand is omitted for clarity.

shows intrinsic chirality due to the arrangement of the staples. The enantiomers of  $\text{Au}_{38}(\text{SCH}_2\text{CH}_2\text{Ph})_{24}$  have been separated by high performance liquid chromatography.<sup>12</sup> Drastic surface reorganization was induced by heating, and a complete racemization of  $\text{Au}_{38}$  can be observed at 80 °C. The effects of support, ligand removal, and gas treatment on catalytic behavior of  $\text{Au}_{38}$  are therefore intriguing. Unlike in the case of  $\text{Au}_{25}$ , thermal treatment of  $\text{CeO}_2$ -supported  $\text{Au}_{38}$  in  $\text{O}_2$  suggests that the catalytic CO oxidation is favored before ligand removal. The catalytic activity of  $\text{Au}_{38}$  is suppressed after the thiolate deprotection.<sup>8</sup>

In this study, we investigated the catalytic activity of  $\text{Au}_{38}(\text{SR})_{24}$  clusters on two metal oxide supports for aerobic oxidation of cyclohexane with a focus on the pretreatment effect. The effect of support and atmosphere on  $\text{Au}_{38}$  thermal treatment was investigated by TG, TPRDO-MS, and XAFS. Both  $\text{Au}_{38}$  and  $\text{Au}_{38}/\text{CeO}_2$  show a two-step weight loss under oxidation atmosphere but only one step in inert atmosphere. In

the treatment under  $\text{O}_2$ ,  $\text{H}_2$ , and He of  $\text{Au}_{38}/\text{Al}_2\text{O}_3$  and  $\text{Au}_{38}/\text{CeO}_2$ , TPRDO-MS revealed a two-step desorption of ligands, possibly corresponding to types of Au–S binding modes. This is clearly shown in the case of  $\text{Au}_{38}/\text{CeO}_2$  under  $\text{H}_2$  and He, where two clear peaks between 175 and 350 °C related with the thiol ligand are observed. EXAFS study clearly revealed the different metal–support interaction for  $\text{Al}_2\text{O}_3$  and  $\text{CeO}_2$ . After complete ligand removal at 300 °C, cationic and metallic gold are observed in  $\text{Au}_{38}/\text{CeO}_2$  and  $\text{Au}_{38}/\text{Al}_2\text{O}_3$ , respectively. Higher catalytic activity is observed in aerobic oxidation of cyclohexane by the stronger metal support interaction and the exposed active Au site.

## ■ EXPERIMENTAL SECTION

### Synthesis of Supported $\text{Au}_{38}(\text{SR})_{24}/\text{M}_x\text{O}_y$ Catalysts.

$\text{Au}_{38}(\text{SR})_{24}$  clusters were synthesized and separated using the method reported previously.<sup>13,14</sup> The synthesized  $\text{Au}_{38}(\text{SR})_{24}$  nanoclusters were characterized by both UV–vis absorption and matrix-assisted laser desorption ionization mass spectrometry (MALDI-MS). For preparation of the  $\text{Au}_{38}(\text{SR})_{24}/\text{M}_x\text{O}_y$  (including  $\text{Al}_2\text{O}_3$  and  $\text{CeO}_2$ ) catalysts, 40 mg of  $\text{Au}_{38}(\text{SR})_{24}$  was dissolved in 100 mL of methylene chloride, and 2 g of the oxide support was added. The mixture was stirred for 10 h at room temperature until the solution was colorless. The solid was collected by filtration and dried.

**Au Cluster Characterization.** UV–vis spectra were recorded on a Varian Cary 50 spectrometer. Quartz cuvettes of 10 or 5 mm path length were used (solvents: methylene chloride and toluene). MALDI-TOF mass spectra were obtained on a Shimadzu Biotech Axima mass spectrometer in linear mode. DCTB was used as a matrix.

**TGA and TPRDO-MS Analysis.** Thermogravimetric analysis (TGA) was performed on STA 449 F3 Jupiter (NETZSCH) under different atmosphere ( $\text{N}_2$  and air) from 25 to 550 °C at a ramp rate of 5 °C/min. MS measurements were obtained with a Pfeiffer OmniStar GSD 320 using the SEM detector. Temperature ramp experiments were conducted in a Thermo TPDRO 1100. The samples (49 mg) were pretreated with 20 sccm of  $\text{N}_2$  or He at room temperature for 2 h. Experiments consisted of heating from room temperature to 400 °C at 10 °C/min with a flow rate of 20 sccm. The gases used were  $\text{N}_2$  (Air Products, purity 5.2) for pretreatment, He (Air Products, purity 5.7) for pretreatment and TPD, 5% of  $\text{H}_2$  in  $\text{N}_2$  (Linde) for TPR, and 5% of  $\text{O}_2$  in He (Air Products) for TPO.

**XAFS Studies.** X-ray absorption (XAFS) measurements at the Au  $L_3$ -edge (11.92 kV) were carried out at the Super-XAS beamline at the Swiss Light Source (Villigen, Switzerland). The samples were filled in a capillary tube and then heated at 100, 200, and 300 °C for 0.5 h and cooled to 25 °C. The spectra were measured in fluorescence mode. XAFS data were treated by IFEFFIT. The fitting procedure was performed on the  $k_2$ -weighted FT-EXAFS from 2 to 10 Å<sup>−1</sup>. A two-shell EXAFS (Au–S and Au–Au) fit was performed for the supported  $\text{Au}_{38}(\text{SR})_{24}/\text{M}_x\text{O}_y$  spectra. A FT-EXAFS  $R$  window of 1 to 3 Å was used for the fitting. The  $S_0^2$  was fixed at 0.864 (deduced from the fitting of Au foil), and all other parameters ( $E_0$ ,  $R$ , and  $\sigma^2$ ) were allowed to run free.

**Thermal Treatment of Supported  $\text{Au}_{38}(\text{SR})_{24}/\text{M}_x\text{O}_y$  Catalysts.** Supported  $\text{Au}_{38}(\text{SR})_{24}/\text{M}_x\text{O}_y$  nanoclusters were thermally treated at 150 and 250 °C under air for 0.5 h. Heating and cooling rates were maintained at 10 °C/min.

**Catalytic Test.** Aerobic oxidation of cyclohexane was performed under solvent-free conditions. An amount of 100 mg of catalyst (2% wt Au) was employed in each run, and 80  $\mu\text{L}$  of TBHP (*tert*-butyl hydroperoxide) was added to 10 mL of cyclohexane in a round glass reactor of 50 mL volume.  $\text{O}_2$  flow of 2.5 mL/min was controlled by a mass flow controller during the reaction. Temperature was kept at 75  $^\circ\text{C}$  with an oil bath with a temperature controller. The quantification and identification of reactant and products was determined by gas chromatography (GC) and a GC-mass spectrometer.

## RESULTS AND DISCUSSION

Thiolate-protected cluster  $(\text{Au}_{38}(\text{SR})_{24})$  supported catalysts were prepared based on previous reports.<sup>12,13</sup> The details about synthesis and separation are described in the Experimental Section. The high purity of the sample was confirmed by UV-vis spectra and MALDI that shows the characteristic bands and masses (see Supporting Information). Gold clusters were immobilized on the surfaces ( $\text{CeO}_2$  and  $\text{Al}_2\text{O}_3$ ) from a dichloromethane solution until the solution was completely colorless. The final product was recovered by filtration and drying at 80  $^\circ\text{C}$ .

**TGA Studies.** In order to gain insights into the effect of thermal treatment on the cluster, several studies by TG (thermogravimetry), TPRDO (temperature-programmed reduction/desorption/oxidation), and XAFS (X-ray absorption spectroscopy) have been performed. The first approach is to study the calcination range required to remove the thiol ligands around the metal core of  $\text{Au}_{38}(\text{SR})_{24}$  by TG under two different atmospheres, inert and air (Figure 2). The weight loss of around 30% (theoretical value 30.56%) between 200 and 270  $^\circ\text{C}$  was observed under an inert atmosphere, which is related to removal of thiolate ligands from the gold cluster, in good agreement with previous studies.<sup>6</sup> However, under air atmosphere, two steps of mass loss are observed. We observed a first weight loss of around 27% between 175 and 240  $^\circ\text{C}$ , followed by a second loss of 11.5% between 240 and 375  $^\circ\text{C}$ . These two steps of mass reduction under oxidation atmosphere were also observed before by A. Shivhare et al.<sup>9</sup> but on  $\text{Au}_{25}$  clusters supported on carbon. It was ascribed to Au clusters catalyzing the oxidation of the carbon support. However, in our case the two steps are also observed with an unsupported cluster. It could be related to interaction of the oxidative atmosphere with the thiol ligands leading to different removal processes.

For supported clusters the interaction of the thiol ligand with the material should affect the desorption process. Figure 2 shows the TG profiles of the  $\text{Au}_{38}(\text{SR})_{24}$  (2 wt %) supported on  $\text{Al}_2\text{O}_3$  and  $\text{CeO}_2$  with the corresponding blank analysis (support without cluster) in both atmospheres (air and inert).

In the case of the  $\text{Al}_2\text{O}_3$ -supported cluster, no clear features related to the thiol ligand are observed. However, different weight loss profiles in the case of air are obtained between the blank and the catalysts. The weight loss related to the thiol ligand in this case could be ascribed to the shoulder at the DTG graphic between 200 and 250  $^\circ\text{C}$  (Supporting Information). The effect of the atmosphere during the thermal treatment can be denoted in the case of supported  $\text{Au}_{38}$  on  $\text{CeO}_2$ . Thiol removal is observed between 150 and 275  $^\circ\text{C}$  under air, whereas under an inert atmosphere the desorption signal extends until around 300  $^\circ\text{C}$ . In both cases a mass loss of 0.8% is observed, which corresponds to removal of 30% of the thiol ligands of 2 wt % of gold clusters on the surface.

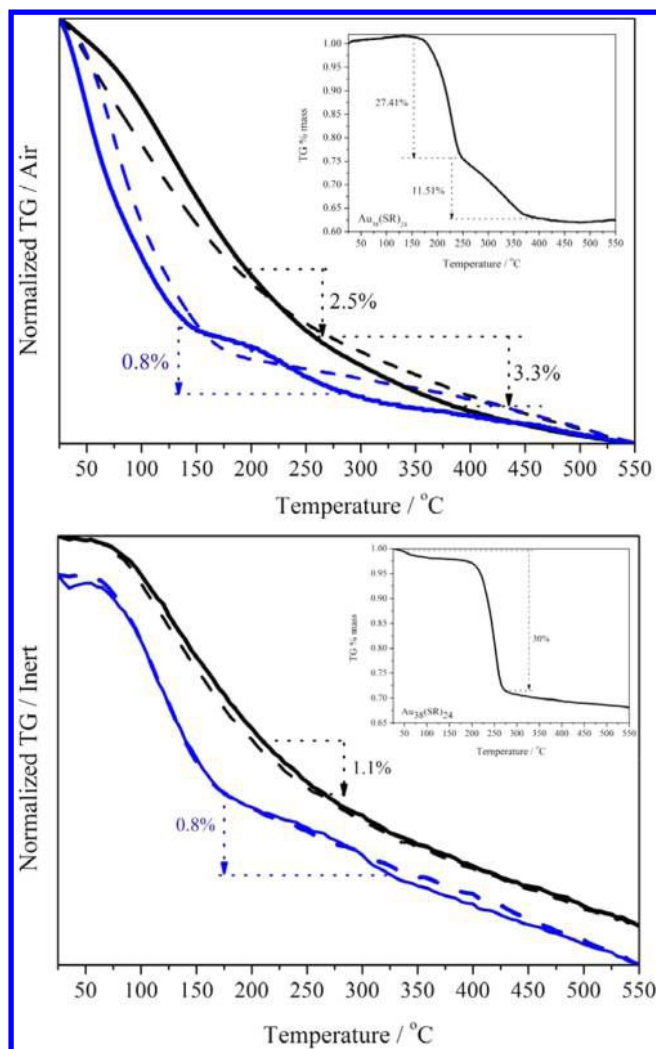


**Figure 2.** TG profiles of  $\text{Au}_{38}(\text{SR})_{24}$  catalysts supported on  $\text{Al}_2\text{O}_3$  (black) and  $\text{CeO}_2$  (blue) in air and an inert atmosphere. Dashed lines correspond to the support alone. Inset: corresponds to the unsupported  $\text{Au}_{38}(\text{SR})_{24}$  cluster.

**TPR/D/O-MS Studies.** In order to better understand the different steps observed in the TG profiles depending on the support and the atmosphere, TPRDO coupled with mass spectrometer analysis was performed. Representative masses related to the thiol ligand fragmentation were monitored during the thermal treatment (91:  $-\text{SC}_8\text{H}_9$ ; 78:  $-\text{C}_6\text{H}_5$ ; 64 and 48: S compounds).

Thiol ligand representative mass (91) is slightly observed starting at 150  $^\circ\text{C}$  and increases strongly from 350  $^\circ\text{C}$  in the case of  $\text{Au}_{38}$  supported on  $\text{Al}_2\text{O}_3$ . Treatments under  $\text{H}_2$  and He atmosphere lead to the same behavior, whereas the sample treated under  $\text{O}_2$  showed a different pattern with small peaks between 250 and 350  $^\circ\text{C}$ . The most intense peaks of mass 78 are present, related to the aromatic ring from the ligand. On the other hand, focusing on the sulfur-related compounds, the center peak is observed between 100 and 275  $^\circ\text{C}$ , indifferent of the atmosphere treatment. Following the pattern of the sulfur compound, mass 64 indicates removal of the thiol ligand from the cluster supported on  $\text{Al}_2\text{O}_3$  up to 300  $^\circ\text{C}$ . However, mass 91 ascribed to the entire thiol ligand is observed to increase at even higher temperatures. This could be related with two-step desorption of the ligands due to different Au–S interactions



from the different staple configurations. Previous NMR studies on  $\text{Au}_{25}(\text{SR})_{18}$  thermal stability have shown that there are two types of Au–S binding modes with different thermal stabilities.<sup>10</sup> A two-step process is observed most clearly in the case of  $\text{Au}_{38}(\text{SR})_{24}$  supported on  $\text{CeO}_2$  (Figure 3, right) under hydrogen and helium: two clear peaks between 175 and 350 °C ascribed to the thiol ligand are observed.

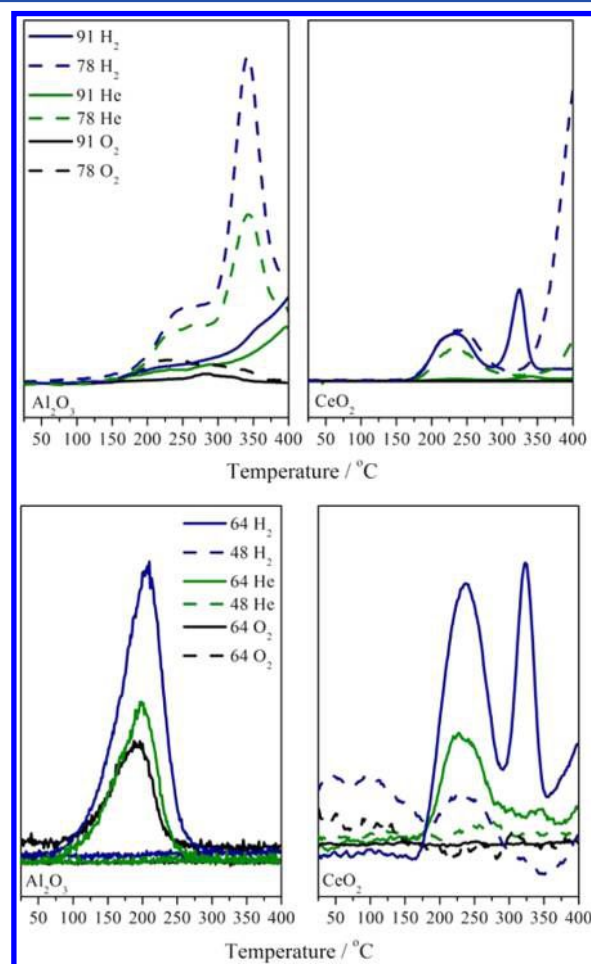


**Figure 3.** Mass spectrometry signals of TPR/D/O profiles of the  $\text{Au}_{38}(\text{SR})_{24}$  catalysts supported on  $\text{Al}_2\text{O}_3$  and  $\text{CeO}_2$  under different atmospheres with a heating rate of 10 °C/min.

**In Situ XAFS Studies.** Changes on the gold core of the  $\text{Au}_{38}(\text{SR})_{24}$  are expected under thermal treatment. The stability of the metal structure and electronic configuration of the cluster were studied by XAFS at the SuperXAS beamline of the Swiss Light Source (SLS) at the Au  $L_3$ -edge in fluorescence mode. The *in situ* measurements of the supported catalysts were performed in a flow cell under oxygen. The sample was heated to the target temperature and after 15 min cooled down for the analysis in order to avoid temperature interferences.

XANES spectrum for the  $\text{Au}_{38}(\text{SR})_{24}$  supported on  $\text{Al}_2\text{O}_3$  and  $\text{CeO}_2$  and references of unsupported  $\text{Au}_{38}(\text{SR})_{24}$ ; Au foil (metallic) and  $\text{Au}_2\text{O}_3$  (cationic) (room temperature to 300 °C), from 11.91 to 11.94 keV, are shown in Figure 4. The intensity of the “white line” of  $\text{Au}_{38}(\text{SR})_{24}$  is slightly higher and shifted in comparison with the Au foil (metallic) due to partial oxidation from the Au–S bond at the staples, although the major part is in the metallic state. Once the cluster is supported, the white line intensity decreased related with the metallic state,

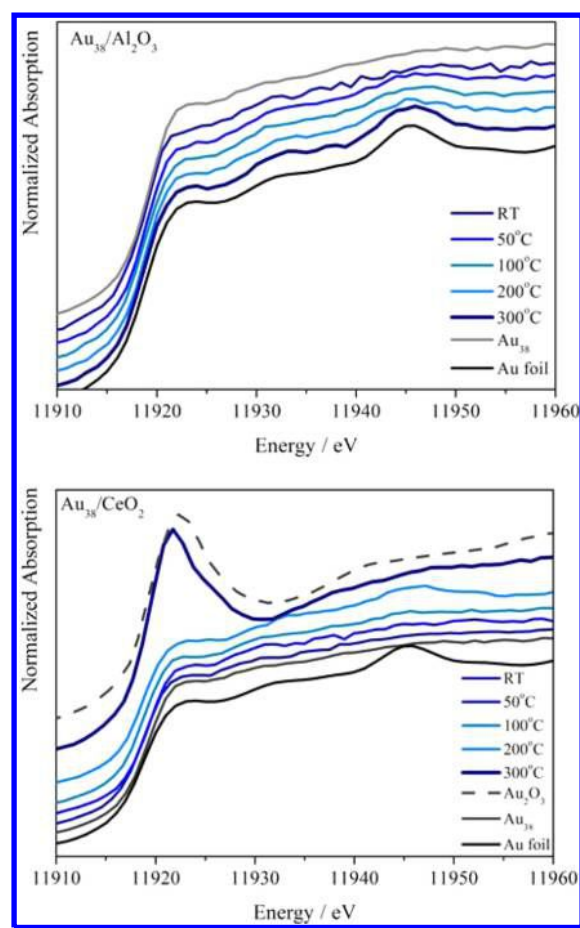


**Figure 4.** Au  $L_3$ -edge XANES spectra of supported  $\text{Au}_{38}(\text{SR})_{24}$  clusters and references under heating.

and upon heating the intensity approached the Au foil intensity level. A striking exception represents the case of the ceria catalyst heated to 300 °C, which shows cationic gold. It could be related to the strong interaction of  $\text{CeO}_2$  with the cluster at high temperatures after losing the thiolate ligands. The presence of cationic Au sites confirmed previous reports<sup>8</sup> on  $\text{Au}_{25}(\text{SR})_{18}$  supported on  $\text{CeO}_2$  treated under  $\text{O}_2$  atmosphere at high temperature and observed by CO adsorption followed by infrared spectroscopy. Z. Wu et al.<sup>8</sup> also performed XAFS studies; however, no cationic state was observed in this case. This was explained by the small fraction of oxidized Au on the surface of the cluster. The different behavior of  $\text{Au}_{38}(\text{SR})_{24}$  and  $\text{Au}_{25}(\text{SR})_{18}$  on  $\text{CeO}_2$  under thermal treatments could be related to structural and electronic differences between the two clusters, which would lead to different interactions with the oxide surface.

EXAFS analysis and fitting for the supported Au cluster under the thermal treatment was performed in order to further study the structural changes focusing on Au–S and Au–Au bonds. Figure 5 shows the EXAFS spectra in  $R$  space for the  $\text{Au}_{38}$  cluster supported on ceria and alumina from room temperature until 300 °C. Below the distance of 2 Å the peak related to the Au–S bond is observed, whereas the peaks above are due to the Au–Au bonds. The spectra of references are also shown for better comparison. It is observed that the Au–S bond length decreases as the temperature increases in agreement with previous studies,<sup>9,15,16</sup> related to the removal of the thiolate ligands. In ceria-supported samples the Au–S

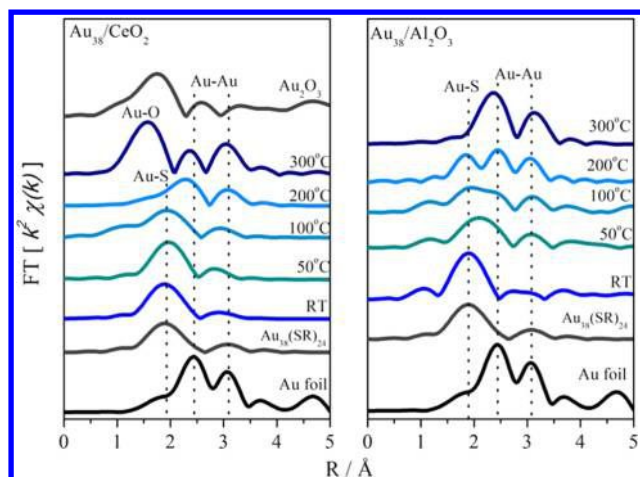


Figure 5. R space spectrum of the  $\text{Au}_{38}$  catalysts and references.

peak is not observed at 300 °C. At this temperature it was only possible to fit the spectra with the  $\text{Au}_2\text{O}_3$  model denoting the cationic state observed in the XANES spectra (Figure 4). In the case of the cluster supported on  $\text{Al}_2\text{O}_3$  at 300 °C the Au–S bond is also not observed; however, in this case the cluster fits with the metallic state. The differences in the behavior of the cluster under thermal treatment depending on the supporting material are due to the interaction of the cluster and thiol ligands with the surface.

The detailed structural parameters were obtained from the spectral multishell fitting of Au–S and Au–Au bonds using a  $\text{Au}_{38}(\text{SR})_{24}$  model compound and  $\text{Au}_2\text{O}_3$  for certain samples. EXAFS fitting parameters obtained are shown in Table 1. Coordination number values for the Au–S bond decrease with temperature increase. The  $\text{Au}_{38}$  cluster on  $\text{CeO}_2$  shows a significant drop at 100 and 200 °C of the Au–S coordination number from 1.31 to 0.30, with a representative increase in the Au–Au CN from 4.60 to 10.69. It is related to the partial removal of thiolate ligands from the Au cluster core, which could imply some sintering of the particle, a fact observed before in the case of  $\text{Au}_{25}$  supported on carbon<sup>9</sup> leading to similar CN values. Higher temperature (300 °C) leads to the Au–O bond related to the cationic state and a further increase in Au–Au CN to 12.84. However, a slight increase in the Au–Au distance is observed, from 2.76 to 2.82 Å, suggesting that the sintering of the cluster is minimal and the particle can be stabilized by the support. In this sense, supporting the Au cluster on reducible oxides such as  $\text{CeO}_2$  leads to strong

interaction with the support once the thiol ligands are removed as evidenced by the Au–O bond but also the stabilization of the cluster.

A different behavior is observed for  $\text{Au}_{38}$  supported on  $\text{Al}_2\text{O}_3$ , where CN of Au–S presents a significant decrease from the fresh sample already at 50 °C (1.48 to 0.72) and the complete removal between 200 and 300 °C. In this step, the Au–Au bond CN increased from 7.21 to 13.20 and the distance from 2.879 to 2.904 Å, suggesting a more representative particle size increase in comparison to the ceria-supported sample. Alumina oxide is a common support material for catalysis without strong interaction with the metals, which could lead to instability of the metal cluster. From XANES results and EXAFS parameters it is observed that once the thiol ligands are removed the metallic state of the Au cluster is obtained, contrary to ceria-supported samples at 300 °C. This is consistent with S. Gaur et al.<sup>15</sup> who studied the reduction treatment of a  $\text{Au}_{38}$  cluster on  $\text{TiO}_2$ . They observed that in fresh catalyst Au is stabilized by the negative charge of support oxide and S from thiol ligands. However, upon removal of the thiol ligand, Au(+1) species decrease, leading to the metallic state of the Au.

It is concluded that depending on the material employed to support the thiolate protected cluster the ligand removal process and the stability of the Au core are affected. Different material properties will lead to different interactions between cluster and support, which will determine the nature of the active surface obtained upon thermal treatments. This represents a key parameter for the catalytic applications of the cluster.

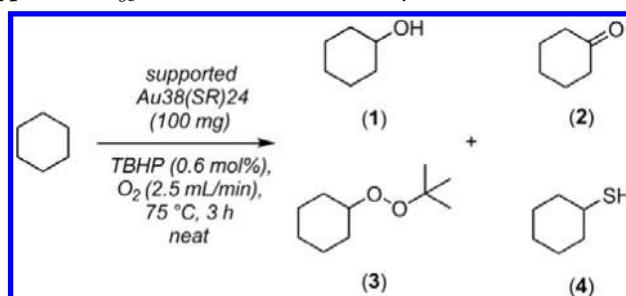
#### Catalytic Activity in Cyclohexane Oxidation Reaction.

The aerobic oxidation reaction of cyclohexane was chosen to observe the effect of the treatment and support materials on the catalytic behavior of  $\text{Au}_{38}$ . Y. Liu et al.<sup>17</sup> studied the particle size effect of supported Au clusters on hydroxyapatite (HPA) and found the highest activity with  $\text{Au}_{39}$  clusters, with 14.9% of cyclohexane conversion and 99% selectivity to cyclohexanol and cyclohexanone. In this case, the protected ligands were removed by calcination before the catalytic test. Recently, another work from the same group (T. Tsukuda)<sup>16</sup> presented the relevant role of the percentage of thiol ligands around the cluster in the catalytic behavior in the aerobic oxidation of benzyl alcohol with  $\text{Au}_{25}$ /carbon catalysts, in terms of activity and selectivity. It was shown that full coverage of the Au cluster by thiol ligands blocks the catalytically active sites, but partial removal of the ligands leads to different product distributions depending on the calcination level. This effect was ascribed to

Table 1. Au  $L_3$  EXAFS Fitting Results

| sample                                 | treatment | bond | CN <sup>a</sup> | R (Å) <sup>b</sup> | $\Delta\sigma^2$ <sup>c</sup> | bond  | CN <sup>a</sup> | R (Å) <sup>b</sup> | $\Delta\sigma^2$ <sup>c</sup> |
|--|-----------|------|-----------------|--------------------|-------------------------------|-------|-----------------|--------------------|-------------------------------|
| $\text{Au}_{38}(\text{SR})_{24}$       | RT        | Au–S | 1.3             | 2.31(4)            | 0.003(2)                      | Au–Au | 3.3             | 2.79(6)            | 0.010(4)                      |
| $\text{Au}_{38}/\text{CeO}_2$          | RT        | Au–S | 1.3(2)          | 2.31(1)            | 0.002(1)                      | Au–Au | 4.6(2)          | 2.76(2)            | 0.016(7)                      |
|  | 50 °C     | Au–S | 1.2(3)          | 2.33(2)            | 0.003(5)                      | Au–Au | 5.2(2)          | 2.72(3)            | 0.012(5)                      |
|  | 100 °C    | Au–S | 0.7(4)          | 2.31(1)            | 0.004(2)                      | Au–Au | 7.5(3)          | 2.76(2)            | 0.016(2)                      |
|  | 200 °C    | Au–S | 0.3(2)          | 2.27(3)            | 0.006(5)                      | Au–Au | 10.7(2)         | 2.85(1)            | 0.001(8)                      |
|  | 300 °C    | Au–O | 3.1(1)          | 1.97(9)            | 0.003(1)                      | Au–Au | 12.8(1)         | 2.82(1)            | 0.008(2)                      |
| $\text{Au}_{38}/\text{Al}_2\text{O}_3$ | RT        | Au–S | 1.5(4)          | 2.31(1)            | 0.003(1)                      | Au–Au | 5.1(3)          | 2.70(2)            | 0.017(7)                      |
|  | 50 °C     | Au–S | 0.8(2)          | 2.38(1)            | 0.003(2)                      | Au–Au | 6.9(6)          | 2.88(1)            | 0.014(1)                      |
|  | 100 °C    | Au–S | 0.7(3)          | 2.31(9)            | 0.002(3)                      | Au–Au | 7.0(1)          | 2.87(7)            | 0.012(2)                      |
|  | 200 °C    | Au–S | 0.7(1)          | 2.30(2)            | 0.002(7)                      | Au–Au | 7.2(2)          | 2.87(2)            | 0.01(2)                       |
|  | 300 °C    | Au–S | --              | --                 | --                            | Au–Au | 13.2(2)         | 2.90(1)            | 0.011(2)                      |

<sup>a</sup>Coordination number. <sup>b</sup>Bond length. <sup>c</sup>Relative Debye–Waller factor.

Table 2. Catalytic Activity of Supported Au<sub>38</sub> and Pretreated in the Cyclohexane Oxidation Reaction

| catalysts  | treatment | cyclohexane conversion | selectivity |       |      |       | KA    |
|--|-----------|------------------------|-------------|-------|------|-------|-------|
|  |           |                        | 1           | 2     | 3    | 4     |       |
| Au <sub>38</sub> /CeO <sub>2</sub>               | RT        | 16.3%                  | 51.7%       | 21.3% | 5.0% | 22.0% | 73.0% |
|  | 150 °C    | 16.8%                  | 55.3%       | 19.8% | 7.5% | 17.3% | 75.1% |
|  | 250 °C    | 39.1%                  | 56.8%       | 22.4% | 5.9% | 14.9% | 79.1% |
| Au <sub>38</sub> /Al <sub>2</sub> O <sub>3</sub> | RT        | 9.5%                   | 9.5%        | 3.6%  | 8.6% | 81.8% | 13.1% |
|  | 150 °C    | 12.0%                  | 13.3%       | 4.9%  | 3.5% | 78.3% | 18.2% |
|  | 250 °C    | 14.2%                  | 16.1%       | 7.5%  | 3.8% | 72.6% | 23.6% |

the reduced oxidation ability of the Au<sub>25</sub> cluster by electron withdrawal, avoiding the esterification reaction in the benzyl alcohol oxidation. On the other hand, X. Nie et al.<sup>6</sup> observed higher activity in CO oxidation with thiol ligands on a Au<sub>38</sub> cluster supported on CeO<sub>2</sub>, pretreated below 100 °C. The same reaction was studied before by Gaur et al.<sup>15</sup> with Au<sub>38</sub>/TiO<sub>2</sub> catalysts, and catalytic activity was only obtained once the thiol ligands were removed. The studies mentioned above reveal the importance of the nature of oxide support, which will lead to different interactions and different ligand removal mechanisms as discussed above in the thermal and XAFS studies results.

Table 2 summarizes the catalytic activity and selectivity of Au<sub>38</sub>(SR)<sub>24</sub> clusters supported on CeO<sub>2</sub> and Al<sub>2</sub>O<sub>3</sub> after different pretreatments in the cyclohexane oxidation reaction. The neat reaction (solvent free) time was established for 3 h under O<sub>2</sub> flow at 75 °C, and TBHP was added in order to initiate the reaction following previous studies.<sup>17–19</sup> Control experiments performed without gold only show the formation of the intermediate cyclohexyl-*t*-butyl peroxide (CyOOT-Bu (3)) due to the presence of TBHP. Clearly, the presence of the Au cluster is required to perform the catalytic reaction. For all the samples, cyclohexane consumption is observed leading to cyclohexanol (1) and cyclohexanone (2) (KA), as well as the intermediate cyclohexyl-*t*-butyl peroxide (3) and unexpected cyclohexanethiol (4). The formation of 4 is directly related to the thiol ligands from the Au cluster, which is further confirmed by the decrease of 4 with a higher temperature treated catalyst, due to the removal of thiol ligands. Cyclohexane consumption is also affected in this way in both cases (Al<sub>2</sub>O<sub>3</sub> and CeO<sub>2</sub>), reflecting the higher number of exposed gold active sites, leading to increased consumption from 16% to 39% in the case of CeO<sub>2</sub> and from 9% to 14% with Al<sub>2</sub>O<sub>3</sub>.

Different catalytic behaviors of the Au<sub>38</sub> cluster are observed depending on the temperature treatment and the support material. In the case of CeO<sub>2</sub> both high yields to desired KA (ketone-alcohol) products and overall conversion are obtained in comparison with Al<sub>2</sub>O<sub>3</sub> catalyst. It could be related to the state of Au (cationic/metallic) upon treatment observed by XAFS analysis. Cationic Au is highly reactive for oxidation reactions. A previous study on CO oxidation reaction has shown the increase in the reactivity with Au clusters supported on ceria in the cationic state.<sup>8</sup> Additional strong effects could be

the support properties; CeO<sub>2</sub> is a reducible oxide with highly reactive vacancies on the surface and with high stabilization effect of metal particles. M. S. Chen et al.<sup>20</sup> showed the influence of support on activity mechanism including stabilization of nanoparticles, formation of active oxygen-containing reactant intermediates, or stabilization of optimal Au structures. Defect sites on oxide supports were shown to play an important role in the wetting of Au particles, yielding electron-rich Au, which is crucial for activating molecular O<sub>2</sub>.<sup>20</sup>

Another relevant point is the unexpected formation of cyclohexanethiol, which varies from a range of 15–22% in CeO<sub>2</sub> to 72–81% with Al<sub>2</sub>O<sub>3</sub>. The possible formation of 4 could be related to two different sources of thiol: residual ligand on the cluster or ligands adsorbed on the support surface reminiscent from the pretreatment process. The reaction selectivity to product 4 decreased upon higher temperature treatment due to the larger number of ligands removed from the cluster, but in the case of Al<sub>2</sub>O<sub>3</sub> catalysts, even at 250 °C, 72% of selectivity is obtained. One open question remains, whether 4 represents a product or an intermediate of the reactions. Further studies on this point are required by longer time reactions and *in situ* infrared spectroscopy measurements, which represent the next step of our research.

## CONCLUSIONS

The creation and modulation of active catalytic sites on thiolate-protected Au<sub>38</sub>(SC<sub>2</sub>H<sub>4</sub>Ph)<sub>24</sub> clusters by thermal treatment in different atmospheres and by supporting on Al<sub>2</sub>O<sub>3</sub> and CeO<sub>2</sub> has been studied. Desorption of the thiolate from the cluster depends on the gas atmosphere and is a complex multistep process. This is particularly evident for the cluster supported on CeO<sub>2</sub> heated in reducing atmosphere, which shows two distinct peaks associated with thiolate fragments during the heating process. Upon heating to 300 °C cationic gold is observed for the cluster supported on CeO<sub>2</sub>, which is however not observed on Al<sub>2</sub>O<sub>3</sub>. The effect of the support and the pretreatment is also evidenced in the catalytic oxidation of cyclohexane. The pretreated catalysts were more active than the untreated ones, showing that the removal of thiolates creates more (efficient) active sites. The clusters supported on CeO<sub>2</sub> were more active than the ones on Al<sub>2</sub>O<sub>3</sub> and showed larger selectivity for ketone and alcohol. On both catalysts formation



of unexpected cyclohexanethiol was observed, which shows that the thiolate is not only blocking and/or modifying catalytic sites but also may take an active part in the catalysis.

## ■ ASSOCIATED CONTENT

### ● Supporting Information

Characterization of synthesized  $\text{Au}_{38}(\text{SR})_{24}$  cluster (UV, MALDI) and TG-DTG profiles of supported catalysts. This material is available free of charge via the Internet at <http://pubs.acs.org>.

## ■ AUTHOR INFORMATION

### Corresponding Authors

\*Noelia Barrabés: [noelia.barrabes@unige.ch](mailto:noelia.barrabes@unige.ch). Phone: +43 (1) 58801 165 109.

\*Thomas Bürgi: [thomas-buergi@unige.ch](mailto:thomas-buergi@unige.ch). Phone: +41(0) 22 379 65 52.

### Notes

The authors declare no competing financial interest.

## ■ ACKNOWLEDGMENTS

NB is grateful to The Swiss National Foundation for the Marie Heim-Vögtlin grant (PMPDP2\_145512). BZ thanks The China Scholarship Council (No. 201306340012). Support from The Swiss National Science Foundation is acknowledged for financial support (grant number 200020\_152596 and project number PP00P2\_133482). The authors acknowledge Swiss Light Source for beamtime at the SuperXAS beamline (Proposal ID: 20130765) and Olga Safonova and Maarten Nachtegaal for assistance with XAS measurements and fitting data. We thank Daniele Poggiali for the GC-mass analysis from the group of Prof. J. Lacour (University of Geneva).

## ■ REFERENCES

- (1) Yamazoe, S.; Koyasu, K.; Tsukuda, T. Nonscalable Oxidation Catalysis of Gold Clusters. *Acc. Chem. Res.* **2014**, *47*, 816–824.
- (2) Li, G.; Qian, H. F.; Jin, R. C. Gold Nanocluster-Catalyzed Selective Oxidation of Sulfide to Sulfoxide. *Nanoscale* **2012**, *4*, 6714–6717.
- (3) Nie, X. T.; Qian, H. F.; Ge, Q. J.; Xu, H. Y.; Jin, R. C. CO Oxidation Catalyzed by Oxide-Supported  $\text{Au}_{25}(\text{SR})_{18}$  Nanoclusters and Identification of Perimeter Sites as Active Centers. *ACS Nano* **2012**, *6*, 6014–6022.
- (4) Das, S.; Goswami, A.; Hesari, M.; Al-Sharab, J. F.; Mikmekova, E.; Maran, F.; Asefa, T. Reductive Deprotection of Monolayer Protected Nanoclusters: An Efficient Route to Supported Ultrasmall Au Nanocatalysts for Selective Oxidation. *Small* **2014**, *10*, 1473–8.
- (5) Knoppe, S.; Bürgi, T. Chirality in Thiolate-Protected Gold Clusters. *Acc. Chem. Res.* **2014**, *47*, 1318–1326.
- (6) Nie, X. T.; Zeng, C. J.; Ma, X. G.; Qian, H. F.; Ge, Q. J.; Xu, H. Y.; Jin, R. C.  $\text{CeO}_2$ -Supported  $\text{Au}_{38}(\text{SR})_{24}$  Nanocluster Catalysts for CO Oxidation: A Comparison of Ligand-on and -Off Catalysts. *Nanoscale* **2013**, *5*, 5912–5918.
- (7) Yoskamtorn, T.; Yamazoe, S.; Takahata, R.; Nishigaki, J.-i.; Thivasasith, A.; Limtrakul, J.; Tsukuda, T. Thiolate-Mediated Selectivity Control in Aerobic Alcohol Oxidation by Porous Carbon-Supported  $\text{Au}_{25}$  clusters. *ACS Catal.* **2014**, *4*, 3696–3700.
- (8) Wu, Z.; Jiang, D. E.; Mann, A. K. P.; Mullins, D. R.; Qiao, Z. A.; Allard, L. F.; Zeng, C.; Jin, R.; Overbury, S. H. Thiolate Ligands as a Double-Edged Sword for CO Oxidation on  $\text{CeO}_2$  Supported  $\text{Au}_{25}(\text{SCH}_2\text{CH}_2\text{Ph})_{18}$  Nanoclusters. *J. Am. Chem. Soc.* **2014**, *136*, 6111–22.
- (9) Shivhare, A.; Chevrier, D. M.; Purves, R. W.; Scott, R. W. J. Following the Thermal Activation of  $\text{Au}_{25}(\text{SR})_{18}$  Clusters for Catalysis by X-Ray Absorption Spectroscopy. *J. Phys. Chem. C* **2013**, *117*, 20007–20016.
- (10) Wu, Z. K.; Jin, R. C. Stability of the Two Au-S Binding Modes in  $\text{Au}_{25}(\text{SG})_{18}$  Nanoclusters Probed by NMR and Optical Spectroscopy. *ACS Nano* **2009**, *3*, 2036–2042.
- (11) Qian, H. F.; Eckenhoff, W. T.; Zhu, Y.; Pintauer, T.; Jin, R. C. Total Structure Determination of Thiolate-Protected  $\text{Au}_{38}$  Nanoparticles. *J. Am. Chem. Soc.* **2010**, *132*, 8280–8281.
- (12) Dolamic, I.; Knoppe, S.; Dass, A.; Bürgi, T. First Enantioseparation and Circular Dichroism Spectra of  $\text{Au}_{38}$  Clusters Protected by Achiral Ligands. *Nat. Commun.* **2012**, *3*, 798.
- (13) Knoppe, S.; Dharmaratne, A. C.; Schreiner, E.; Dass, A.; Bürgi, T. Ligand Exchange Reactions on  $\text{Au}_{38}$  and  $\text{Au}_{40}$  Clusters: A Combined Circular Dichroism and Mass Spectrometry Study. *J. Am. Chem. Soc.* **2010**, *132*, 16783–16789.
- (14) Knoppe, S.; Boudon, J.; Dolamic, I.; Dass, A.; Bürgi, T. Size Exclusion Chromatography for Semipreparative Scale Separation of  $\text{Au}_{38}(\text{SR})_{24}$  and  $\text{Au}_{40}(\text{SR})_{24}$  and Larger Clusters. *Anal. Chem.* **2011**, *83*, 5056–5061.
- (15) Gaur, S.; Miller, J. T.; Stellwagen, D.; Sanampudi, A.; Kumar, C. S. S. R.; Spivey, J. J. Synthesis, Characterization, and Testing of Supported Au Catalysts Prepared from Atomically-Tailored  $\text{Au}_{38}(\text{SC}_{12}\text{H}_{25})_{24}$  Clusters. *Phys. Chem. Chem. Phys.* **2012**, *14*, 1627–1634.
- (16) Yoskamtorn, T.; Yamazoe, S.; Takahata, R.; Nishigaki, J. I.; Thivasasith, A.; Limtrakul, J.; Tsukuda, T. Thiolate-Mediated Selectivity Control in Aerobic Alcohol Oxidation by Porous Carbon-Supported  $\text{Au}_{25}$  Clusters. *ACS Catal.* **2014**, *4*, 3696–3700.
- (17) Liu, Y. M.; Tsunoyama, H.; Akita, T.; Xie, S. H.; Tsukuda, T. Aerobic Oxidation of Cyclohexane Catalyzed by Size-Controlled Au Clusters on Hydroxyapatite: Size Effect in the Sub-2 Nm Regime. *ACS Catal.* **2011**, *1*, 2–6.
- (18) Xu, L. X.; He, C. H.; Zhu, M. Q.; Fang, S. A Highly Active  $\text{Au}/\text{Al}_2\text{O}_3$  Catalyst for Cyclohexane Oxidation Using Molecular Oxygen. *Catal. Lett.* **2007**, *114*, 202–205.
- (19) Xu, Y. J.; Landon, P.; Enache, D.; Carley, A.; Roberts, M.; Hutchings, G. Selective Conversion of Cyclohexane to Cyclohexanol and Cyclohexanone Using a Gold Catalyst under Mild Conditions. *Catal. Lett.* **2005**, *101*, 175–179.
- (20) Chen, M. S.; Goodman, D. W. Structure–Activity Relationships in Supported Au Catalysts. *Catal. Today* **2006**, *111*, 22–33.